cyte localization in hematomas: a pitfall in abscess detection. *Radiology* 1984;152: 173–176.
20. Chung CJ, Wilson AA, Melton JW, et al. Uptake of In-111 labeled leukocyte by lymphocele. A cause of false-positive vascular graft infection. *Clin Nucl Med* 1992;17:368–369.
21. Serota AI, Williams RA, Rose JG, et al. Uptake of radiolabeled leukocytes in prosthetic graft infection. *Surgery* 1981;90:35–40.
22. Roddie ME, Peters AM, Danpure HJ, et al. Inflammation with Tc-99m-HMPAO-labeled leukocytes. *Radiology* 1988;166:767–772.
23. Mark A, Moss AA, Lusby R, et al. CT evaluation of complication of abdominal aortic surgery. *Radiology* 1982;145:409–414.
24. Vogelzang RL, Limpert JD, Yao JS. Detection of prosthetic vascular complication: comparison of CT and angiography. *Am J Roentgenol* 1987;148:819–823.
25. Johnson KK, Russ PB, Bair JH, Friefeld GD. Diagnosis of synthetic vascular graft infection: comparison of CT and gallium scan. *Am J Roentgenol* 1990;154:405–409.
26. Fiorani P, Speziale F, Rizzo L, et al. Detection of aortic graft infection with leukocytes labeled with technetium 99m-hexametazime. *J Vasc Surg* 1993;17:87–96.

Dexamethasone Treatment and Plasma Glucose Levels: Relevance for Fluorine-18-Fluorodeoxyglucose Uptake Measurements in Gliomas

Ulrich Roelcke, Ronald G. Blasberg, Klaus von Ammon, Silvia Hofer, Peter Vontobel, Ralph P. Maguire, Ernst W. Radü, Richard Herrmann and Klaus L. Leenders

PET Program, Paul Scherrer Institute, Villigen, Switzerland; Memorial Sloan Kettering Cancer Center, New York, New York; Department of Neurosurgery, University Hospital, Zürich, Switzerland; Departments of Oncology and Neuroradiology, University Hospital, Basel, Switzerland; and Department of Neurology, University Hospital, Zürich, Switzerland

Dexamethasone (DEX) is frequently used in brain tumor management. This study investigated the effect of DEX treatment and plasma glucose levels on ^{18}F-fluorodeoxyglucose (FDG) uptake in patients with malignant gliomas (16 glioblastoma, 3 anaplastic astrocytoma). **Methods:** Fifteen DEX-treated patients (mean relative dose 0.23 ± 0.15 $mg^{-1} \cdot kg^{-1} \cdot day^{-1}$, range 0.07–0.53), four patients not treated with DEX and nine healthy subjects were studied using PET and FDG. PET data obtained from tumors and the contralateral cortex were fitted to a standard two-tissue compartment model. The FDG transport and phosphorylation rates, distribution volume (DV), steady-state accumulation (Ki), deoxyglucose metabolism (R), plasma volume as well as standardized uptake values (SUVs) and tumor-to-brain ratios were determined. In addition, the tumor size was estimated from the maximal area of contrast-enhancing tumor on computed cranial tomography (CCT) scans or MRI. **Results:** FDG uptake was depressed in the contralateral cortex of patients and was related to tumor size. With increasing relative DEX dose, a decrease in the DV of tumors (linear regression $p = 0.021$) and in the DV ($p = 0.109$) and plasma volume ($p = 0.010$) of contralateral cortex was found. R, Ki and SUVs in tumors and contralateral cortex were not related to the relative DEX dose. With increasing plasma glucose levels, differential decreases in Ki and SUVs in tumors ($p = 0.057$ and $p = 0.733$, respectively) and contralateral cortex ($p = 0.001$ and $p = 0.029$, respectively) were observed. **Conclusion:** The data suggest that DEX affects FDG uptake in malignant gliomas through interaction with cerebral blood vessels and extracellular space, whereas FDG metabolism in tumors is not influenced substantially. This is of practical importance for patients having serial brain tumor imaging for treatment evaluation because patients may receive different DEX doses at different time points in the course of their disease. By contrast, the plasma glucose level must be considered a confounding variable when SUVs, tumor-to-brain ratios or Ki are used for treatment evaluation.

Key Words: malignant glioma; dexamethasone; plasma glucose; PET; fluorine-18-fluorodeoxyglucose

J Nucl Med 1998; 39:879–884

Received Feb. 1, 1997; revision accepted Aug. 6, 1997.

For correspondence or reprints contact: K.L. Leenders, MD, PET Program, Paul Scherrer Institute, CH 5232 Villigen, Switzerland.

Dexamethasone (DEX) is widely used in treating brain tumors (*1*). Most patients with malignant brain tumors receive DEX for treatment of brain edema. It also is administered to prevent brain swelling during brain tumor irradiation. In addition, because DEX sensitivity has been observed in primary central nervous system lymphomas, it is recommended as part of the cytolytic drug regimen in these tumors (*2*).

The cytolytic effects of DEX are considered to be mediated by glucocorticoid receptors (GCRs) [for a review, see Norgaard and Poulsen (*3*)]. In gliomas, studies evaluating the presence of GCRs have produced controversial results. Surgical specimens of human glioma patients have revealed values ranging from 0% (*4*) to 100% (*5*) GCR-positive tumor cells. Conflicting data also were reported concerning the effect of DEX treatment, which could induce both growth inhibition (*6,7*) and growth stimulation (*8,9*) of glioma cell lines. Moreover, in rats bearing intracerebral 9L gliomas, DEX increased the number of tumor blood vessels exhibiting glucose transporter (*10*) and changed the phenotype of malignant tumor cells toward a higher degree of differentiation (*7*). It is not clear how these experimental findings relate to the situation of DEX-treated human brain tumor patients in situ. In this study, we used PET to investigate the influence of DEX on ^{18}F-fluorodeoxyglucose (FDG) uptake in malignant brain tumors and the cerebral cortex contralateral to the tumor. FDG PET has been used previously to assess brain tumor malignancy (*11*), therapy response (*12*) and dedifferentiation (*13*). Because DEX treatment may induce hyperglycemia, which in turn may influence FDG uptake in glioma patients (*14*), we also assessed the relationship between plasma glucose levels and FDG uptake parameters.

MATERIALS AND METHODS

FDG PET data from 19 patients with histologically proven supratentorial malignant gliomas were analyzed retrospectively. Fifteen patients (aged 53 ± 12 yr, mean ± s.d.) were DEX treated: 12 glioblastomas (GBMs) World Health Organization (WHO) IV and 3 anaplastic astrocytomas WHO III; $n = 11$ at first presentation and $n = 4$ at the time of recurrence after combined radiochemotherapy. DEX was administered orally to all patients. The mean daily DEX dose was 16 ± 10 mg (range 4–32 mg/day); the dose

at the time of the PET investigation had been stable for at least 4 days preceding the study. The daily dose was normalized for body weight, yielding a relative daily DEX dose of 0.23 ± 0.15 $mg^{-1} \cdot kg^{-1} \cdot day^{-1}$ (range 0.07–0.53). Four GBM patients (aged 58 ± 18 yr and not statistically different from DEX-treated patients) did not receive DEX because of stable disease after combined radiochemotherapy, which was clinically and neuroradiologically documented at the time of the PET investigations. The daily dose of anticonvulsants in both groups was not statistically different (carbamazepin: DEX treated 254 ± 357 mg, not DEX treated 225 ± 250 mg; phenytoin: DEX treated 197 ± 159 mg, not DEX treated 250 ± 354 mg). Nine healthy individuals (6 men, 3 women; aged 48 ± 12 yr) served as controls. Permission to perform PET studies in patients and controls was given by the ethics committees at the university hospitals of Basel and Zürich.

Scanning Procedure

Patients were positioned parallel to the orbitomeatal line with the tumor (as shown on CCT scans or MRI) in the center of the field of view. The head was placed in an individually molded thermoplastic head support to minimize movement during scanning. After a 10-min transmission scan ($^{68}Ga/^{68}Ge$ ring source), dynamic PET scans were performed on a CTI machine (933/04-16, four rings, seven planes, 8-mm FWHM) immediately after an intravenous injection of 140–298 MBq FDG. A time frame schedule of 3 × 60, 10 × 180 and 3 × 300 sec was used, resulting in a total scan duration of 48 min. Nineteen blood samples were manually drawn from an indwelling catheter placed in the radial artery. In addition, five arterial blood samples were drawn immediately before and during the PET studies to determine plasma glucose levels.

Data Analysis

Elliptical regions of interest (ROIs) were placed over the whole tumor, with the ROI size and position being determined by visual comparison with the corresponding contrast-enhanced CCT scan or MRI. On the brain side contralateral to the tumor, elliptical ROIs were placed over the cortex opposite to the tumor. ROI time-activity curves and plasma input data were fitted to a standard two-tissue compartment model using a nonlinear least squares algorithm (*15*). This procedure results in an estimate of rate constants (k), where K1 [ml/g/min] denotes tracer influx from plasma into the tissue precursor compartment, k2 denotes [1/min] tracer efflux from the precursor compartment back to the plasma, and k3 [1/min] denotes tracer "trapping" in an irreversible compartment. In the case of FDG, k3 reflects the phosphorylation rate of FDG by hexokinase. From these rate constants, the distribution volume (DV) of free FDG in tissue (K1/k2 [ml/g]) and the steady-state accumulation (Ki; K1*k3/(k2 + k3) $[ml^{-1} \cdot g^{-1} \cdot min^{-1}]$ (*16*)) of FDG input was calculated. The steady-state condition (in which the plasma FDG input and tissue FDG accumulation are in equilibrium) is considered to be present 40–60 min after FDG injection. By calculating cerebral glucose metabolism (CMR_{glu}) with the two-tissue compartment model at various time points from dynamic PET studies, which were acquired over 120 min, Lucignani et al. (*17*) showed that CMR_{glu} became constant 30 min after injection. More than 60 min after injection, dephosphorylation of FDG-6-phosphate (k4) may increasingly contribute to the loss of tissue radioactivity.

From Ki, CMR_{glu} of normal brain can be derived easily using the plasma glucose concentration and a fixed lumped constant value (*18*). In individual tumors, the lumped constant may vary considerably and is not known (*19*). In this study, we used deoxyglucose metabolism (R) of tumors and contralateral brain, which was calculated as Ki* plasma glucose concentration. The regional plasma volume (%) also was estimated in the fit of the dynamic PET data. The error associated with the fitting procedure was expressed for each parameter as the coefficient of variation (CV) in percent [s.d. divided by the fitted value (%CV)].

For tumor and contralateral brain, standardized uptake values (SUVs) also were calculated using the last time frame of the time-activity curves (48 min after tracer injection) as ROI activity concentration over injected dose per gram body weight (becquerels per milliliter per becquerels per gram). In addition, the SUV ratios of tumor over contralateral cortex were calculated.

We also estimated the tumor size, which was assumed to correspond to the tumor area calculated from the axial plane (computed crania tomography (CCT) scan or MRI, available as films) showing the greatest contrast-enhancing tumor diameter. From that plane, the largest diameter of the contrast-enhancing tumor was determined (x). Vertical to that line, a second diameter was determined (y). The tumor size was then calculated as the elliptical area in the following equation:

$$\pi * \frac{x}{2} * \frac{y}{2} \ (mm^2).$$

Statistical Analysis

Group-to-group differences were tested using the Mann–Whitney test. A possible correlation between FDG uptake parameters and the relative DEX dose, plasma glucose levels or tumor size was tested using Spearman's rank correlation coefficient.

RESULTS

All tumors were visible on the PET images as lesions with at least somewhat higher FDG accumulation in tumors than in the corresponding brain contralateral to the tumors. The estimated parameters for FDG accumulation in tumors and the contralateral cortex and for cortex of normal subjects are shown in Table 1. Mean errors associated with parameter estimation (%CV) were higher in tumors than in the contralateral cortex and may reflect the greater heterogeneity of tumor tissue (see the note to Table 1).

FDG accumulation in the contralateral cortex of tumor patients was compared with that in the comparable cortex of healthy control individuals (Table 1). Metabolism (R) and the steady-rate accumulation (Ki) of FDG were significantly lower in cortex of tumor patients than in healthy control subjects (R and Ki: $p < 0.001$). SUV values also were lower in the cortex of tumor patients, but this difference did not reach statistical significance. K1 and K3 values were marginally lower in the cortex of tumor patients than in healthy control subjects.

FDG accumulation parameters (R, Ki, SUV and tumor-to-contralateral cortex ratio) in tumors and the contralateral cortex were compared with tumor size. In tumors, no correlation between tumor size and any of these parameters was found. In the contralateral cortex, increasing tumor size was associated with decreasing R (Fig. 1).

FDG accumulation also was compared in DEX-treated and nontreated patients (Table 1). Significantly lower R values were found in the contralateral cortex of DEX-treated patients than in nontreated patients ($p = 0.036$). SUV and Ki values in the contralateral cortex also were lower in DEX-treated patients, but this difference did not reach statistical significance (SUV $p = 0.162$, Ki $p = 0.267$) because of the large variation in SUV and Ki values. In tumors, the mean values of R, Ki and SUV were virtually the same in both DEX-treated and nontreated patients. K1 and k3 were similar in DEX-treated and nontreated patients for tumors and the contralateral cortex. On average, k2 was higher in tumors and the contralateral cortex for DEX-treated patients (contralateral cortex $p = 0.064$). Accordingly, the DV was lower in DEX-treated patients (the difference for

TABLE 1
FDG Uptake in Tumors and Contralateral Cortex in Patients and Uptake in Control Subjects

Parameters	Tumor		Contralateral cortex		Healthy controls
	DEX+ (n = 15)	DEX− (n = 4)	DEX+ (n = 15)	DEX− (n = 4)	DEX− (n = 9)
K1 ml/g/min	0.074 ± 0.022	0.078 ± 0.015	0.072 ± 0.021	0.069 ± 0.017	0.083 ± 0.011
k2 liter/min	0.133 ± 0.059	0.114 ± 0.036	0.126 ± 0.048*	0.089 ± 0.020	0.125 ± 0.049
k3 liter/min	0.061 ± 0.027	0.058 ± 0.021	0.044 ± 0.011	0.053 ± 0.009	0.088 ± 0.027
DV ml/g	0.601 ± 0.180	0.732 ± 0.246	0.613 ± 0.197†	0.795 ± 0.181	0.753 ± 0.203
Ki ml/g/min	0.023 ± 0.007	0.026 ± 0.011	0.019 ± 0.005	0.026 ± 0.009	0.034 ± 0.004¶
R μmol/g/min	0.152 ± 0.050	0.154 ± 0.028	0.125 ± 0.026‡	0.156 ± 0.020	0.199 ± 0.011¶
V_p %	6.3 ± 3.8	5.0 ± 1.9	4.3 ± 1.2§	5.4 ± 0.6	4.7 ± 0.6
SUV Bq/ml per Bq/g	4.9 ± 1.5	5.1 ± 1.8	4.0 ± 0.9	5.2 ± 1.8	5.9 ± 1.5
T/C ratio	1.23 ± 0.30	0.98 ± 0.17			

Significance levels for differences in FDG uptake parameters between contralateral cortex of DEX+ vs. DEX− patients (Mann Whitney).
*p = 0.064.
†p = 0.057.
‡p = 0.036.
§p = 0.083.
Significance levels for differences between contralateral cortex in all 19 glioma patients and cortex in healthy subjects.
¶p = 0.001.
FDG uptake parameters in DEX-treated (DEX+) and non-treated (DEX−) patients with malignant brain tumors and in normal healthy controls. K1, k2, k3 = rate constants; DV = distribution volume (K1/k2); Ki = steady-state accumulation of FDG; R = deoxyglucose metabolism; V_p = plasma volume; SUV = standardized uptake value; T/C ratio = tumor-to-contralateral cortex ratio. Values are given as mean ± 1s.d. Mean errors associated with parameter estimation in tumors (TU) and contralateral cortex (CL): K1 = 11% ± 5% (TU), 6% ± 4% (CL); k2 = 19% ± 9% (TU), 13% ± 5% (CL); k3 = 14% ± 12% (TU), 9% ± 4% (CL); V_p = 23% ± 19% (TU), 19% ± 15% (CL).

contralateral cortex: p = 0.057). The plasma volume in the contralateral cortex (but not in tumors) also tended to be lower in DEX-treated patients (p = 0.083). SUVs were correlated with Ki in tumors and the contralateral cortex (ρ = 0.674, p < 0.001); SUVs also correlated with R (ρ = 0.619, p < 0.001) and DV (ρ = 0.451, p = 0.005).

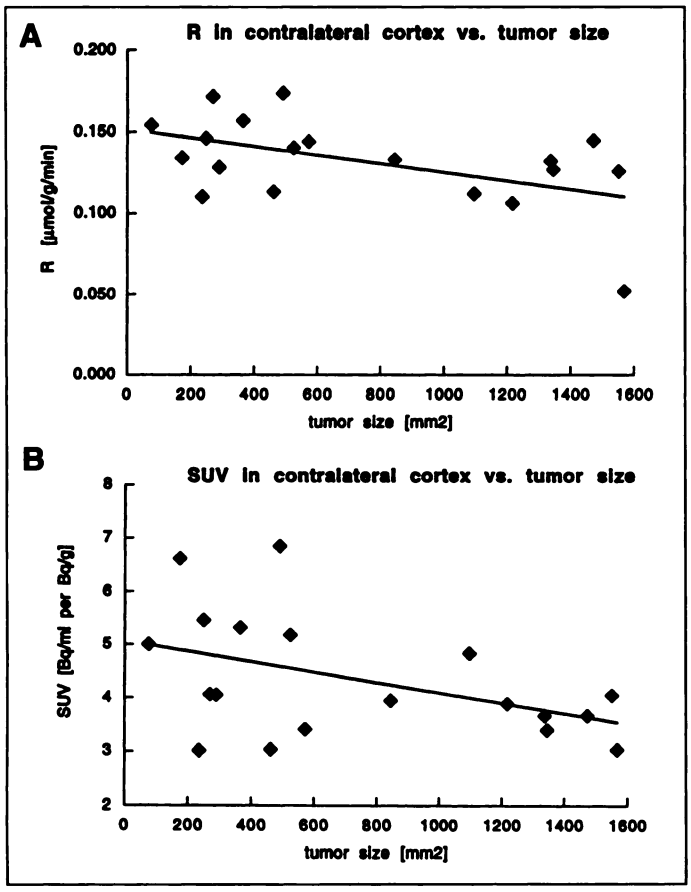

FIGURE 1. Relationship between tumor size and FDG accumulation (R, SUV) in the cortex contralateral to the tumor side. (A) R: ρ = −0.439, p = 0.063; linear regression: r = 0.151–6.5*10^{-6} * tumor size, regression coefficient r = −0.505, p = 0.028. (B) SUV: ρ = −0.438, p = 0.063; linear regression: SUV = 5.06–2.4*10^{-4} * tumor size, r = −0.448, p = 0.055.

The tumor size was, on average, higher in DEX-treated (841 ± 549 mm^2) than in nontreated patients (376 ± 186 mm^2). The dose of DEX (milligrams per day) was not correlated with any of the FDG uptake parameters, but the relative dose of DEX (normalized to body weight [milligram per kilogram per day]) did correlate with tumor DV (Fig. 2A). A similar trend was observed for the contralateral cortex (Fig. 2B). Neither R nor Ki of FDG in tumors and the contralateral cortex was related to the relative DEX dose (R: tumor, ρ = −0.013, p = 0.959; contralateral cortex, ρ = −0.320, p = 0.244; Ki: tumor, ρ = −0.027, p = 0.913; contralateral cortex, ρ = −0.336, p = 0.159). The plasma volume in the contralateral cortex (but not in tumors) decreased with increasing relative DEX doses (ρ = −0.575, p = 0.010). SUVs in tumors or the contralateral cortex were not correlated with the relative DEX dose.

Plasma glucose levels (expressed as the average value of five samples) were 6.7 ± 1.3 mmol/liter (range 5.1–9.4) in DEX-treated patients and 6.2 ± 1.3 mmol/liter (range 4.4–7.4) in nontreated patients. No correlation between the relative DEX dose and plasma glucose levels (ρ = −0.059, p = 0.726) was found. Not surprisingly, an inverse correlation between tumor Ki of FDG and plasma glucose levels was observed (Fig. 3A). In the contralateral cortex, this correlation was more evident (Fig. 3B). As expected, metabolism (R) and plasma glucose were not correlated in tumors (ρ = 0.214, p = 0.378) or the contralateral cortex (ρ = −0.167, p = 0.494). Tumor SUVs were not correlated with plasma glucose (Fig. 4A), whereas contralateral cortex SUVs decreased with increasing plasma glucose levels (Fig. 4B). In the contralateral cortex, further correlations between FDG uptake parameters and plasma glucose levels were found for K1 (ρ = −0.459, p = 0.048), k3 (ρ = −0.532, p = 0.019) and the DV (ρ = −0.523, p = 0.021).

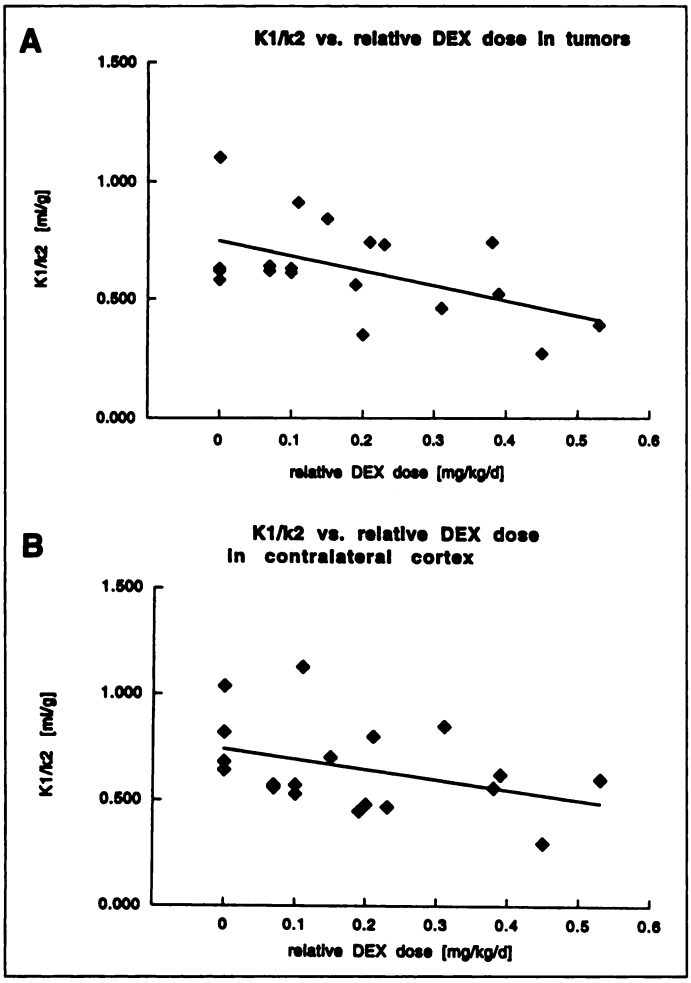

FIGURE 2. Relationship between relative DEX dose and distribution volume of free FDG in tissue (K1/k2). (A) Tumors: $\rho = -0.525$, p = 0.021; K1/k2 = 0.745–0.636 * relative DEX dose, r = −0.525, p = 0.021. (B) Contralateral cortex: $\rho = -0.379$, p = 0.109; K1/k2 = 0.739–0.476 * relative DEX dose, r = −0.379, p = 0.109).

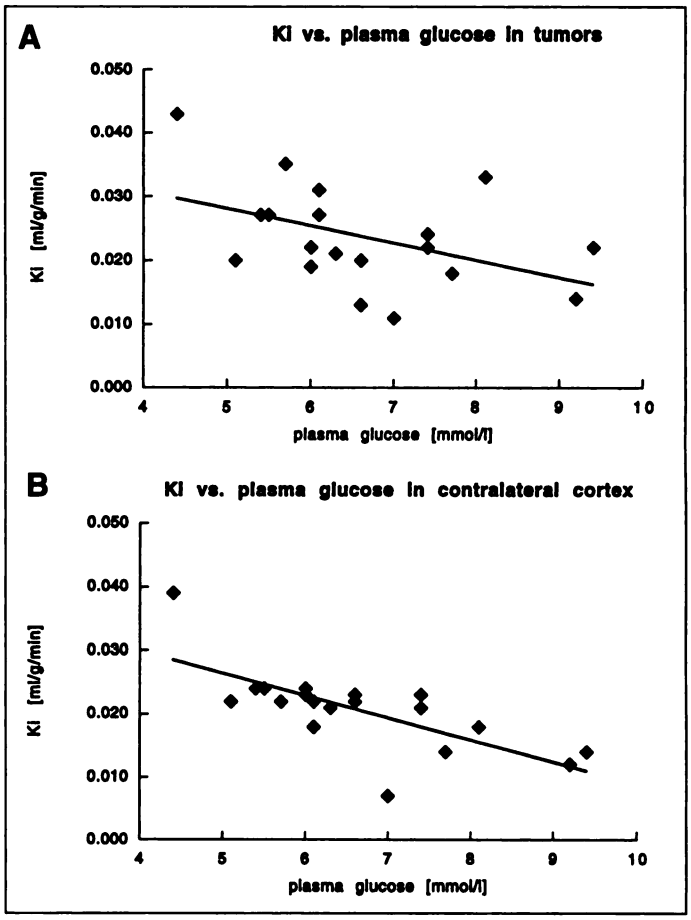

FIGURE 3. Relationship between plasma glucose levels and steady-state accumulation of FDG (Ki). (A) Tumors: $\rho = -0.443$, p = 0.057; Ki = 0.041–0.027 * plasma glucose, r = −0.443, p = 0.057. (B) Contralateral cortex: $\rho = -0.713$, p = 0.001; Ki = 0.044–0.035 * plasma glucose, r = −0.713, p < 0.001.

DISCUSSION

Our results define the kinetics of FDG accumulation in patients with malignant brain tumors relative to DEX treatment. As has been reported earlier (*20,21*), we found that FDG metabolism (R) and steady state accumulation (Ki) in the cortex contralateral to the tumors of patients was significantly lower than that of the comparable cortex in healthy, normal individuals. We extend this observation by defining a relationship between metabolism in the contralateral cortex and tumor size (Fig. 1). Taking the weak correlation between DEX dose and contralateral glucose metabolism into account, our results suggest that reductions in contralateral glucose metabolism are dominated by tumor size and that DEX treatment adds—at best—only little to this reduction. Surprisingly, no tumor differences were observed between DEX-treated and nontreated patients in any of the FDG model parameters (R, Ki, SUV, DV, K1, k2, k3 and plasma volume), and there was no correlation in tumors between R, Ki or SUV values and the relative DEX dose.

A recent FDG PET study showed lower glucose metabolism in the contralateral brain of DEX-treated patients (*22*). Among the DEX-treated group, 14 of 16 patients suffered from malignant gliomas, whereas in the nontreated group, only 12 of 29 were malignant gliomas. Because malignant brain tumors themselves may suppress energy metabolism of the contralateral brain (*20,21*), the overrepresentation of these tumors in the DEX treatment group may have contributed to the lower glucose metabolism measured in this group. In our series, only malignant brain tumors were studied. R, Ki and SUV values were lower in the contralateral cortex of DEX-treated patients, but only the differences in R were significant. As suggested earlier, we attribute these reductions to the tumor size itself. Consistent with this interpretation, DEX treatment was found not to have any effect on oxygen use, an alternative measure of energy metabolism, which has been measured with PET and $^{15}O_2$ in brain tumors and the contralateral brain immediately before and after administration of DEX (*23*). Note that the previously mentioned FDG PET studies (*20–22*) and our study were based on interindividual comparisons. FDG PET studies before and after initiation of DEX treatment in the same patient would be helpful in establishing whether DEX affects the glucose metabolism of tumors and brain tissue. However, these studies would be difficult to perform because the accepted clinical practice is to administer corticosteroids to patients suspected of having a high-grade brain tumor. Early corticosteroid treatment may effectively exclude the availability of patients to study the effects of DEX on tumor and brain glucose metabolism.

Our results did demonstrate an inverse relationship between the physiological DV (K1/k2) of FDG and DEX treatment (expressed as the relative daily DEX dose) in malignant brain tumors and the contralateral cortex. The plasma volume also was found to decrease with increasing relative DEX doses in the cortex contralateral to the tumor site. A possible explanation for

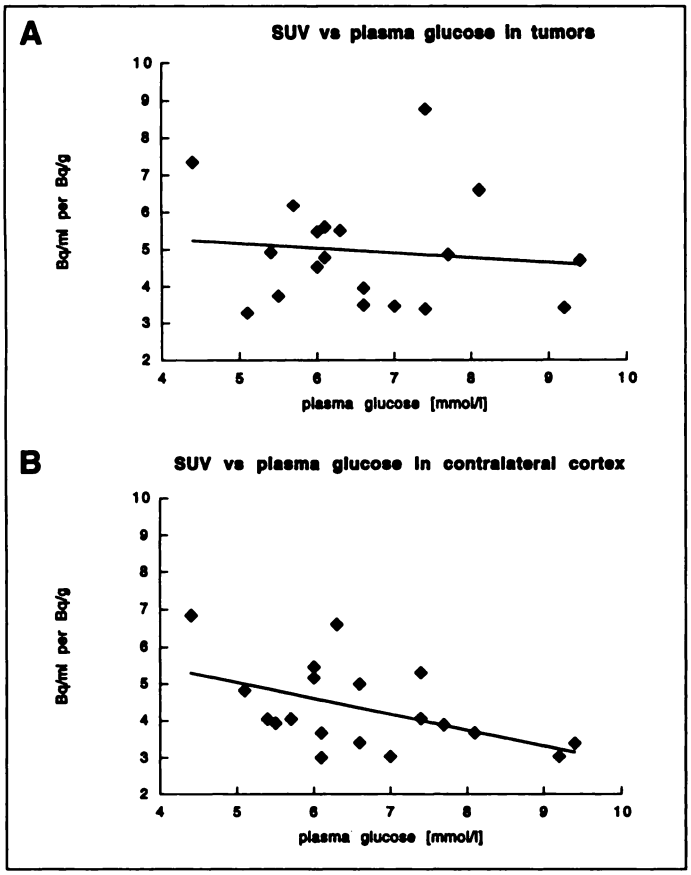

FIGURE 4. Relationship between plasma glucose levels and SUVs. (A) Tumors: $\rho = -0.081$, p = 0.733; SUV = 5.8–0.128 * plasma glucose, r = −0.113, p = 0.645. (B) Contralateral cortex: $\rho = -0.449$, p = 0.029; SUV = 6.8–0.388 * plasma glucose, r = −0.436, p = 0.062.

the observed effects of DEX on the physiological DV are its interactions with the vasculature and with the extracellular space. One PET study (using $H_2{}^{15}O$ and $C^{15}O$) demonstrated blood flow and blood volume reductions in brain tumors and the contralateral cortex after DEX administration (16–20 mg daily) (*23*). This was attributed to vasoconstriction, which could result from the inhibition of prostacyclin release from endothelial cells caused by DEX treatment (*24*). In addition, the DEX effect on the tumor DV could relate to a steroid-induced reduction in the size of extracellular space (*25,26*). A smaller extracellular space would result in a lower DV for FDG. This is reflected in the rate constants, in which the average k2 was higher in our DEX-treated patients, giving rise to an average lower DV in those patients.

Studies in animals (*27*) and healthy humans (*28*) have demonstrated a close correlation between glucose supply and metabolic demands. In addition, because of the competition between unlabeled glucose and FDG at the blood-brain barrier glucose transporter and the hexokinase enzyme, an inverse relation between the plasma glucose concentration and the rate constants K1 and k3 can be expected. Our data clearly show this for the contralateral cortex but not for tumors. Similar findings have been reported by Herholz et al. (*29*), who also found an uncoupling between FDG transport and phosphorylation in tumors. Our results are consistent with these data, suggesting that significant interindividual variations of tumor K1 and k3 may abolish the inverse relationship between competing plasma glucose and FDG rate constants, which is observed in the normal brain.

In clinical practice, where arterial blood samples are frequently not available, brain tumor imaging with FDG and PET is commonly assessed by calculating SUVs from tissue radioactivity concentrations, administered FDG dose and body weight (*30*). Alternatively, simple ratios are calculated from radioactivity concentrations in tumors over that in some defined brain region (e.g., contralateral cortex or white matter). Because these measures are usually obtained from later imaging time points (approximately 40–60 min after tracer injection), SUVs and tumor-to-brain concentration ratios are considered to reflect steady state values for FDG. This is supported by the correlation between SUVs and Ki values in tumors and the contralateral cortex (see the Results section). However, intergroup comparison studies based on differences between mean SUVs or tumor-to-brain ratios are likely to be compromised by high intragroup variability. This was found to be true for the data presented in Table 1. The variability (s.d.) of SUVs for the cortex of healthy control individuals was 26% of the mean value, whereas the variability was only 7% for comparable R (Table 1). In addition, the influence of plasma glucose levels on tumor SUVs is usually not considered when comparing sequential studies in individual patients (e.g., measurements pre- and posttreatment). Differences in plasma glucose concentrations during sequential FDG studies in the same patient could result in differences in SUVs and Ki values (*14,29*) as well as changes in the appearance of the images, which do not necessarily reflect changes in glucose metabolism (R).

CONCLUSION

Supratentorial malignant brain tumors depress the glucose metabolism of the contralateral cortex, and the magnitude of this depression correlates with tumor size. The weak correlation between cortical metabolism and DEX dose (normalized to body weight) probably reflects the correlation between tumor size and DEX dose rather than a specific action of DEX on brain glucose metabolism. The results of our study suggest that brain tumor metabolism is not affected by DEX treatment (range 4–32 mg/day) or tumor size. These observations are of practical importance because patients receive different DEX doses at different time points in the course of their disease, and FDG PET scans also are obtained at different stages of their disease.

The optimal FDG accumulation parameter for serial evaluation of glioma patients (e.g., treatment response) is still CMR_{glu} or R. SUV measurements do not account for changes or differences in the arterial input function of blood FDG radioactivity or blood glucose concentration. However, because arterial blood sampling is indispensable for the determination of CMR_{glu} or R, noninvasive procedures such as venous methods or blood glucose indexing should be exploited to make use of the overall practical value of FDG PET imaging. Noninvasive methods could then provide appropriate measures of FDG phosphorylation, also being suitable for serial investigations of glioma patients.

REFERENCES

1. French LA, Galicich JH. The use of steroids for control of cerebral edema. *Clin Neurosurg* 1962;10:212–223.
2. Fine HA. Treatment of primary central nervous system lymphoma: still more questions than answers. *Blood* 1995;86:2873–2875.
3. Norgaard P, Poulsen S. Glucocorticoid receptors in human malignancies: a review. *Ann Oncol* 1991;2:541–557.
4. Rengachary SS, Tilzer JJ. A study of dexamethasone receptor protein in human gliomas. *J Surg Res* 1981;31:447–455.
5. Yu ZY, Wrange Ö, Boëthius J, et al. A study of glucocorticoid receptors in intracranial tumors. *J Neurosurg* 1981;55:757–760.
6. Maciunas RJ, Mericle RA, Sneed CL, Hefner DJ, Commers PA, Kovacs WJ. Determination of the lethal dose of dexamethasone for early passage in vitro human glioblastoma cell cultures. *Neurosurg* 1993;33:485–488.
7. Mackie AE, Freshney RI, Aturk F, et al. Glucocorticoids and the cell surface of human glioma cells: relationship to cytostasis. *Br J Cancer* 1988;58(suppl):101–107.

8. Langeveld CH, van Waas MP, Stoof JC, et al. Implication of glucocorticoid receptors in the stimulation of human glioma cell proliferation by dexamethasone. *J Neurosci Res* 1992;31:524–531.
9. Gibelli N, Zibera C, Butti G, et al. Hormonal modulation of brain tumor growth: a cell culture study. *Acta Neurochir (Wien)* 1989;101:129–133.
10. Guerin C, Wolff JE, Laterra J, Drewes LR, Brem H, Goldstein GW. Vascular differentiation and glucose transporter in rat gliomas: effects of steroids. *Ann Neurol* 1992;31:481–487.
11. Di Chiro G. Positron emission tomography using [^{18}F] fluoro-deoxyglucose in brain tumors: a powerful diagnostic and prognostic tool. *Invest Radiol* 1986;22:360–371.
12. Hölzer T, Herholz K, Jeske J, Heiss WD. FDG-PET as a prognostic indicator in radiochemotherapy of glioblastoma. *J Comput Assist Tomogr* 1993;17:681–687.
13. Francavilla TL, Miletich RS, Di Chiro G, Patronas NJ, Rizzoli HV, Wright DC. Positron emission tomography in the detection of malignant degeneration of low-grade gliomas. *Neurosurgery* 1989;24:1–5.
14. Ishizu K, Nishizawa S, Yonekura Y, et al. Effects of hyperglycemia on FDG uptake in human brain and glioma. *J Nucl Med* 1994;35:1104–1109.
15. Ralston ML, Jennrich RI. Dud, a derivative-free algorithm for non-linear least squares. *Technometrics* 1978;20:7–14.
16. Patlak CS, Blasberg RG, Fenstermacher JD. Graphical evaluation of blood-to-brain transfer constants from multiple-time uptake data. *J Cereb Blood Flow Metabol* 1983;3:1–7.
17. Lucignani G, Schmidt KC, Moresco RM, et al. Measurement of regional cerebral glucose utilization with fluorine-18-FDG and PET in heterogeneous tissues: theoretical considerations and practical procedure. *J Nucl Med* 1993;34:360–369.
18. Phelps ME, Huang SC, Hoffman EJ, et al. Tomographic measurement of local cerebral glucose metabolic rate in humans with [^{18}F]2-fluoro-2-deoxy-d-glucose: validation of method. *Ann Neurol* 1979;6:371–388.
19. Spence AM, Graham MM, Muzi M, et al. Deoxyglucose lumped constant estimated in a transplanted rat astrocytic glioma by the hexose utilization index. *J Cereb Blood Flow Metab* 1990;10:190–198.
20. DeLaPaz RL, Patronas NJ, Brooks RA, et al. PET study of suppression of gray-matter glucose-utilization by brain tumors. *AJNR* 1983;4:826–829.
21. Herholz K, Rudolf J, Heiss WD. FDG transport and phosphorylation in human gliomas measured with dynamic PET. *J Neurooncol* 1992;12:159–165.
22. Fulham MJ, Brunetti A, Aloj L, Raman R, Dwyer AJ, Di Chiro G. Decreased cerebral glucose metabolism in patients with brain tumors: an effect of corticosteroids. *J Neurosurg* 1995;83:657–664.
23. Leenders KL, Beaney RP, Brooks DJ, Lammertsma AA, Heather JD, McKenzie CG. Dexamethasone treatment of brain tumor patients: effects on regional cerebral blood flow, blood volume, and oxygen utilization. *Neurology* 1985;35:1610–1616.
24. Axelrod L. Inhibition of prostacyclin production mediates permissive effect of glucocorticoids on vascular tone. *Lancet* 1983;i:903–906.
25. Luthert PJ, Greenwood. Experimental studies and the blood-brain barrier. In: Capildeo R, ed. *Steroids in diseases of the central nervous system.* New York: Wiley & Sons; 1989;47–57.
26. Nagakawa H, Groothuis DR, Owens ES, Fenstermacher JD, Patlak CS, Blasberg RG. Dexamethasone effect on [^{125}I] albumin distribution in experimental RG-2 gliomas and adjacent brain. *J Cereb Blood Flow Metabol* 1987;7:687–701.
27. Hawkins RA, Mans AM, Davis DW, Hibbard LS, Lu DM. Glucose availability to individual cerebral structures is correlated to glucose metabolism. *J Neurochem* 1983;40:1013–1018.
28. Heiss WD, Pawlik G, Herholz K, et al. Regional kinetic constants and cerebral metabolic rate for glucose in normal human volunteers determined by dynamic positron emission tomography of [^{18}F]2-fluoro-2-deoxy-D-glucose. *J Cereb Blood Flow Metabol* 1984;4:212–223.
29. Herholz K, Ziffling P, Staffen W, et al. Uncoupling of hexose transport and phosphorylation in human gliomas demonstrated by PET. *Eur J Cancer Clin Oncol* 1988;24:1139–1150.
30. Oldendorf WH. Expression of tissue isotope distribution. *J Nucl Med* 1974;15:725–726.

Organ-Specific Insulin Resistance in Patients with Noninsulin-Dependent Diabetes Mellitus and Hypertension

Ikuo Yokoyama, Tohru Ohtake, Shin-ichi Momomura, Katsunori Yonekura, Nobuhiro Yamada, Junichi Nishikawa, Yasuhito Sasaki and Masao Omata

The Second Department of Internal Medicine, the Department of Radiology, and the Third Department of Internal Medicine, University of Tokyo, Tokyo, Japan.

Abnormal heart and skeletal muscle glucose metabolism in diabetes or essential hypertension has been demonstrated. However, the role of hypertension in heart and skeletal muscle glucose utilization in diabetes has not been clarified yet. **Methods:** We compared heart and skeletal muscle glucose utilization using PET and the whole-body glucose disposal rate (GDR) during insulin clamping in 9 patients with noninsulin-dependent diabetes mellitus (NIDDM) and essential hypertension and 11 patients with NIDDM without hypertension to examine the effect of hypertension on heart and skeletal muscle glucose utilization. Results also were compared with those for 8 asymptomatic healthy control participants. **Results:** Skeletal muscle glucose utilization rate was comparable between hypertensive NIDDM patients (61.2 ± 55.5 $\mu mol \cdot min^{-1} \cdot kg^{-1}$) and normotensive NIDDM patients (50.9 ± 25.2 $\mu mol \cdot min^{-1} \cdot kg^{-1}$) but was significantly reduced in both groups compared with control subjects (94.2 ± 57.3 $\mu mol \cdot min^{-1} \cdot kg^{-1}$), as was the GDR (25.2 ± 11.3 and 24.0 ± 7.5 $\mu mol \cdot min^{-1} \cdot kg^{-1}$), respectively, for patients compared with 38.5 ± 11.5 $\mu mol \cdot min^{-1} \cdot kg^{-1}$ for control participants). However, the myocardial glucose utilization (MGU) rate was significantly reduced in NIDDM patients without hypertension (389 ± 185 $\mu mol \cdot min^{-1} \cdot kg^{-1}$) than in those with hypertension (616 ± 86.4 $\mu mol \cdot min^{-1} \cdot kg^{-1}$, $p < 0.01$). Multivariate stepwise regression analysis has shown that MGU was significantly correlated with systolic blood pressure and plasma free fatty acid concentration. **Conclusion:** Whole-body insulin resistance was observed in NIDDM patients independent of hypertension. The MGU rate may have different properties to oppose insulin resistance than glucose utilization of skeletal muscle in hypertensive patients with NIDDM.

Key Words: glucose metabolism; insulin resistance; diabetes mellitus; hypertension; PET; fluorodeoxyglucose

J Nucl Med 1998; 39:884–889

A recent investigation has revealed that reactivity to insulin between heart and skeletal muscle varies among several diseases, some of which usually are thought to be associated with insulin resistance (*1*). Furthermore, it has been suggested that glucose utilization may vary between heart and skeletal muscle according to the specific disorder (*1–3*). For example, there is increased myocardial glucose utilization (MGU) but reduced skeletal muscle glucose utilization (SMGU) in patients with mild hypertension (*1*). Reduced glucose utilization in the heart but preserved skeletal muscle (*2*) also have been reported. These observations strongly suggest that the kinetics of cardiac muscle glucose utilization may be different from that of SMGU in patients with insulin resistance.

Received Mar. 11, 1997; revision accepted Aug. 5, 1997.
For correspondence or reprints contact: Ikuo Yokoyama, MD, 7-3-1 Hongoh Bunkyo-ku, Tokyo 113, Japan.